Cs/Li/O Co-adsorption on GaAs(001)β2 (2×4) surface: a first-principles research

XIAOHUA YU[1,2,*], ZUDE JIN[1,2]
[1]*Shanxi Province Intelligent Optoelectronic Sensing Application Technology Innovation Center, Yuncheng University, Yuncheng,044000, China*
[2]*Shanxi Province Optoelectronic Information Science and Technology Laboratory, Yuncheng University, Yuncheng, 044000, China*

In this work, DFT with plane-wave ultrasoft pseudopotential based on first-principles was used to investigate the Cs/Li-O co-adsorption on the GaAs(001)β2 (2×4) reconstruction surface. Firstly, the structural distortion, stability, and ionicity were analyzed. Subsequently, the photoemission properties were investigated in detail from three perspectives: dipole moment, band structure, and optical properties. Results showed that during Cs only activation and Cs/O activation, the proper introduction of Li atoms could improve the photoemission, but it should be noted that the introduction of too much Li atoms would reduce of photoemission. The optimal ratio of Cs to Li is 4:2 and 5:1 during the Cs only activation and Cs/O activation respectively.

(Received April 24, 2025; accepted April 6, 2026)

Keywords: Cs/Li/O co-adsorption, Work function, Band structure, Optical properties

1. Introduction

As a typical III-V semiconductor materials, GaAs is widely used [1-5]. With high quantum efficiency, low energy spread and high spin polarization, NEA (Negative Electron Affinity) photocathodes made by GaAs are widely used in the weak light detection and are potential electron sources for the next-generation electron accelerators [6,7].

The preparation of photocathodes consists of three procedures: wafer growth, surface clean and surface activation, of which the latter is the most important [8,9]. In a classic activation process, a two-step process consists of Cs only activation process and Cs/O co-activation process, Cs and O atoms cover atomically clean GaAs surface, reducing the work function, achieving the NEA (Negative Electron Affinity) photocathodes [10]. Cesium (Cs) belongs to alkali metal, to enhance the activation effect, Mulhollan et al. conducted experiments to compare the activation performance of various alkali metal atoms on GaAs photocathodes, the results demonstrated that incorporating a specific amount of lithium (Li) atoms during the Cs/O activation process can improve the quantum efficiency of the photocathode [11]. The study of Sun et al. also showed that the quantum efficiency of GaAs photocathode was greatly improved after Li atom was added to the activation process [12]. Liu et al. researched the Cs/Li/NF_3 activation process of GaN nanowire photocathode by first-principles calculation method, and the results showed that the best photoemission properties can be obtained when the Cs: Li ratio is 1:1 [13].

At present, the theoretical study of Cs/Li/O activation process in GaAs cathode is still lacking, and the activation mechanism of Cs/Li/O is still unclear. In this paper, using first-principles [14] calculation method, Cs-O and Cs/Li-O co-adsorption GaAs(001)β2 (2×4) models were built, work function, dipole moment, electron density difference, band structure, DOS (density of state), absorption coefficient and reflectivity of these co-adsorption models are calculated, the influence of Li atom on the Cs/Li-O activation process of GaAs photocathodes were analyzed.

2. Calculation models and calculation method

Cambridge Serial Total Energy Package (CASTEP), based on the density functional theory (DFT) [15], was used in the calculations. The exchange and correlation interactions [16] was treated through Generalized gradient approximation (GGA) [16,17] with the Perdew-Burke-Ernzerhof (PBE) functional. Atomic pseudopotentials, described through Ultrasoft pseudopotential [18,19], were generated from electron states of Ga:3d104s24p1, As:4s24p3, Cs:5s25p66s1,

Li:1s22s1, O:2s22p4 and H:1s. The energy cut off was set as 400eV and the number of k points is 4×6×1. Energy tolerance, force tolerance, stress tolerance and maximum displacement were respectively set as 1×10-5 eV/atom, 0.03 eV/Å, 0.02Gpa and 0.001 Å. GaAs belongs to zinc-blende structure at room temperature and pressure. According to the literature value [20], the lattice parameter of GaAs is taken as 0.56533nm. The calculation of different GaAs(001) reconstruction phases, performed by Weichao Wang et.al. [21], showed that β2 (2×4) was the most stable reconstruction phase, β2 (2×4) phase is chosen in this research. Slab model was used in the calculation and self-consistent dipole correction was performed [22]. Since 7-8 atomic layers is sufficient for getting converged surface properties [23], the reconstruction surface model was built with 7 layers of atoms (there Ga, Al layers and four As layers). During the optimization, atoms at top four layers were relaxed freely while the atoms at bottom three layers are fixed to simulate a bulk environment. There are 22 Ga atoms, and 28 As atoms in the clean surface model. The vacuum thickness of the slab models is set as 1.5nm. The calculated work function of clean GaAs(001)β2 (2×4) model was 4.764eV, consistent well with the literature value 4.9eV [24], showing the reliability of our research.

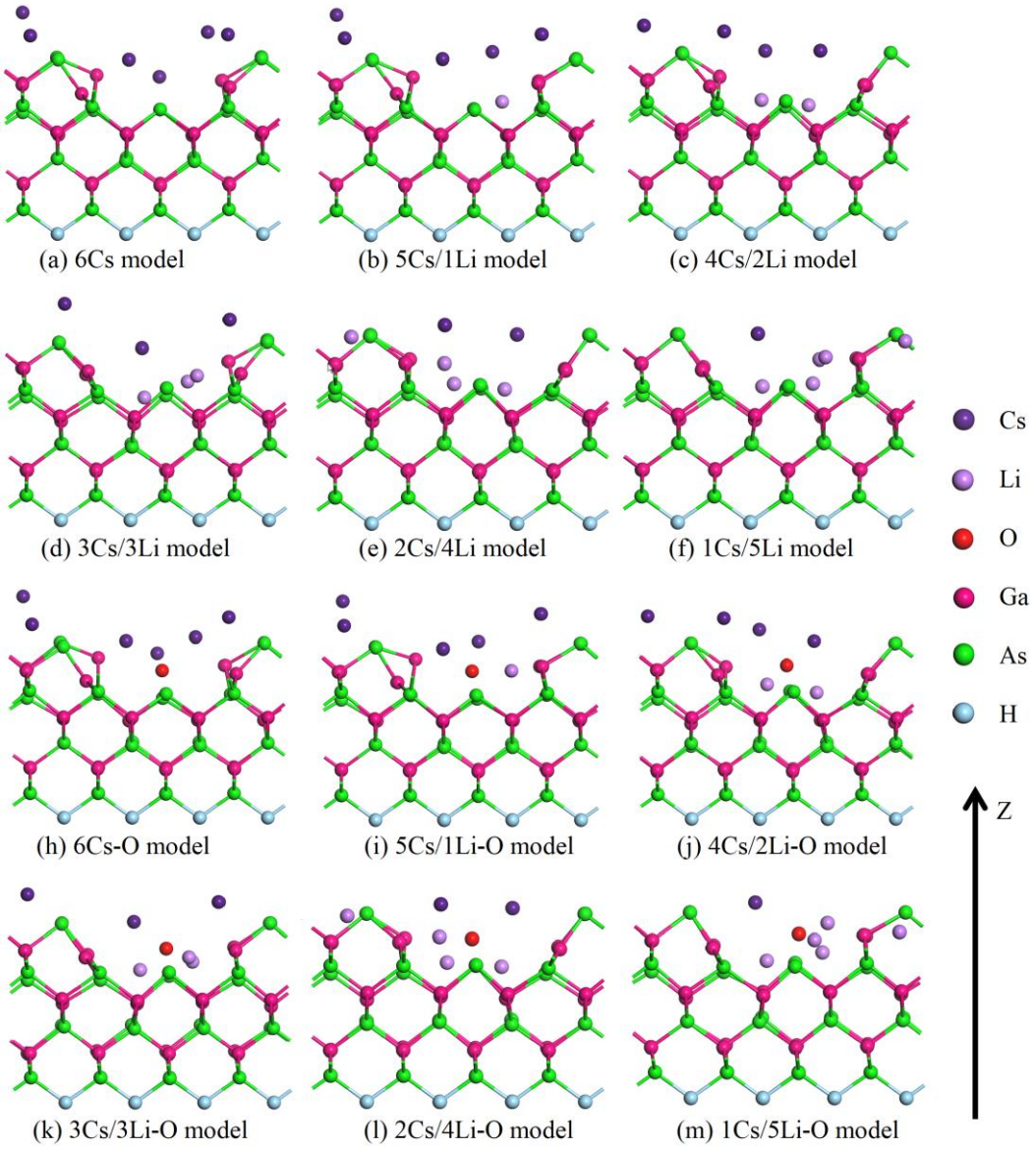

Fig. 1. Calculation models (colour online)

The calculation models were shown in Fig. 1. Firstly, the Cs only activation process was simulate, the results indicated that the work function reached its minimum value when six Cs atoms are adsorbed, which aligned with the experimental findings that the highest quantum efficiency was achieved when Cs coverage was

approximately 0.7 monolayers (ML) [25], therefore, the adsorbed GaAs(001) β2 (2×4) model with 6 Cs atoms was chosen as reference, labeled as 6Cs model in Fig 1 (a), afterwards, 5Cs/1Li, 4Cs/2Li, 3Cs/3Li, 2Cs/4Li and 1Cs/5Li models were built for the research on the influence of Li atoms on the Cs only activation process. Finally, 6Cs-O, 5Cs/1Li-O, 4Cs/2Li-O, 3Cs/3Li-O, 2Cs/4Li-O and 1Cs/5Li-O models were built for the research on the influence of Li atoms on the Cs/O activation process.

3. Results and discussion

3.1. Geometric structure, stability and ionicity

It can be seen from Fig. 1 that compared with Cs atom, Li atom is adsorbed closer from the surface, and there is even one Li atom embedded in GaAs in the 1Cs/5Li-O model. The following formula can be used to study the change of the geometric structure of each model.

$$\Delta l = \sqrt{\sum_{i=1}^{N}[(\Delta x_i)^2 + (\Delta y_i)^2 + (\Delta z_i)^2]} / N \qquad (1)$$

where, Δx_i , Δy_i and Δz_i respectively represent the change in the corresponding coordinate of the atom i in the adsorbed surface compared to the clean surface, i is the number of all Ga and As atoms, N is the total number of Ga and As atoms, N=50. The calculated Δl were shown in Table 1. It can be observed from the computational results that the adsorption of Cs atoms had a significant influence on the surface morphology and atomic positions. The incorporation of Li further intensified the changes in atomic positions. Among the models, 3Cs/3Li model exhibited the most pronounced positional changes, whereas the 4Cs/2Li model demonstrated the least. Additionally, the introduction of O atoms exacerbated the changes in surface atomic positions. Specifically, the 3Cs/3Li-O model showed the greatest positional alteration, while the 5Cs/1Li-O model exhibited the smallest change.

The adsorption energy, used to analyze the stability of the models, can be calculated through the following equation $\Delta H_{Cs/Li\text{-}O} = E_{total} - E_{slab} - N_{Cs}E_{Cs} - N_{Li}E_{Li} - N_O E_O$, where E_{total} , E_{slab} , E_{Cs} , E_{Li} and E_O respectively represent the calculated total energy of the absorption model, the clean surface model, Cs atom, Li atom and O atom, N_{Cs} , N_{Li} and N_O are respectively the number of the Cs, Li and O atoms[26,27]. The calculated adsorption energies of the models were collected in Table 1. Results showed that, the adsorption energies were all negative, showing that the adsorption was an exothermic process, all the models were stable. The addition of O atom increased the stability of each model, showing that the photocathode life after Cs/Li-O activation was longer than Cs/Li only activation. During the Cs/Li co-adsorption and Cs/Li-O co-adsorption processes, the introduction of Li element increased the stability of the model, and with the increase of Li element, the stability of the model gradually increased. This is due to the fact that the radius of the Li atom (1.52 Å) was much smaller than that of the Cs atom (3.34 Å), which was easier to adsorb close to the surface, in the 1Cs/5Li-O model, there were even Li atoms embedded in the GaAs surface. The calculation results showed that the photocathode life can be increased by adding Li element.

Table 1 Atomic position change, adsorption energy, charge-transfer index, work function, charge change, dipole moment of calculation models

model	6Cs	5Cs/1Li	4Cs/2Li	3Cs/3Li	2Cs/4Li	1Cs/5Li	6Cs-O	5Cs/1Li-O	4Cs/2Li-O	3Cs/3Li-O	2Cs/4Li-O	1Cs/5Li-O
Δl (10^{-3}Å)	7.92	9.10	8.52	12.59	9.37	9.65	11.24	11.24	14.38	20.34	12.56	22.28
$\Delta H_{Cs/Li\text{-}O}$	-9.59	-10.6	-12.03	-12.89	-13.24	-14.04	-17.75	-17.75	-18.73	-20.31	-20.44	-21.64
c	0.41	0.384	0.423	0.431	0.422	0.418	0.401	0.401	0.427	0.44	0.441	0.421
Φ (eV)	3.174	3.066	2.986	3.017	3.617	4.017	2.931	2.931	3.026	3.103	3.509	3.851
Δe_{Cs+Li}	3.08	3.67	3.71	4.34	4.4	4.51	3.85	3.85	4.08	4.68	4.78	4.92
μ	-0.899	-0.96	-1.005	-0.987	-0.648	-0.422	-1.036	-1.036	-0.982	-0.939	-0.709	-0.516
$\lvert Q^{\pm}\rvert$ (e)	3.21	3.67	4.64	5	4.66	4.61	4.85	4.85	5.14	5.54	5.44	5.39
d_z (Å)	3.434	3.185	2.841	2.458	1.907	1.414	2.958	2.958	2.369	2.009	1.665	1.279
p_z	11.023	11.689	13.182	12.29	8.887	6.519	14.346	14.346	12.177	11.13	9.058	6.894

Charge-transfer index [28], defined by Paula Mori-Sánchez, provides a measurement of ionicity of the model. It can be obtained by the following formula:

$$c = \frac{1}{N}\sum_{\Omega=1}^{N}\frac{\ell(\Omega)}{OS(\Omega)} = \left\langle \frac{\ell(\Omega)}{OS(\Omega)} \right\rangle \quad (2)$$

where N is the number of atoms in the system, $\ell(\Omega)$ is the topological charge, $OS(\Omega)$ is the nominal oxidation states. The calculated charge-transfer index of clean GaAs(001)β2 (2×4) surface is 0.334. The charge-transfer index of GaAs(001)β2 (2×4) surface in the adsorption models were shown in Table 1. Results showed that the surface ionicity of each adsorption models were stronger than that of clean surface, and the ionicity of oxygen-containing model was stronger than that of oxygen-free model. As the number of Li atoms increases, the ionicity decreases first and then increases. The ionicity of oxygen-free model is 3Cs/3Li, and that of oxygen-containing model is 2Cs/4Li-O.

3.2. Work function, charge transfer and dipole moment

For semiconductors, the work function is defined as the minimum energy needed by electrons in the system to escape externally and can be expressed as $\Phi = E_{vac} - E_F$ [29], where E_{vac} and E_F represent, respectively, the vacuum level and Fermi level. The calculated work function of the adsorption models is collected in Table 1. The work function of clean surface is 4.764eV. The adsorption of 6 Cs atoms reduced the work function to 3.174eV, which improved photoemission significantly. The addition of O atoms further reduced the work function to 2.966eV. In the oxygen-free activation process, the addition of Li atom caused the work function first decreased and then increased, reaching the lowest value at 4Cs/2Li. In the oxygen-containing activation process, the addition of Li atom caused the work function first decreased and then increased, reaching the lowest value at 5Cs/1Li-O model. During Cs only activation and Cs/O activation, the proper introduction of Li atoms could improve the photoemission, but it should be noted that the introduction of too much Li atoms would reduce of photoemission.

The change of work function was mainly caused by the dipole moment formed by the transfer of electrons from Cs and Li atoms to the surface. In order to study the reason for the change of work function, the electronic density difference diagram was depicted in Fig.2, for convenience only electronic density difference of 6Cs, 4Cs2Li, 2Cs4Li, 6Cs-O, 5Cs1Li-O, 2Cs4Li-O models were collected. In the figure, blue indicates the increase of electrons before and after adsorption, and yellow indicates the decrease of electrons. The average charge transfer amount of Cs and Li atoms in each adsorption model was collected in Table 1. Results showed that, the addition of O atoms significantly increased the amount of charge change, thus reducing the work function and promoting photoemission. After a small number of Li atoms replaced Cs atoms, the charge changes at the surface became more obvious, thus reducing the work function. With the increase of Li atoms, the charge at the surface moved towards the surface because Li atoms were closer to the surface, thus increasing the work function and hindering photoemission. This is consistent with the phenomenon that a small number of Li atoms could reduce the work function and increase the photoemission, while too many Li atoms would hinder the photoemission.

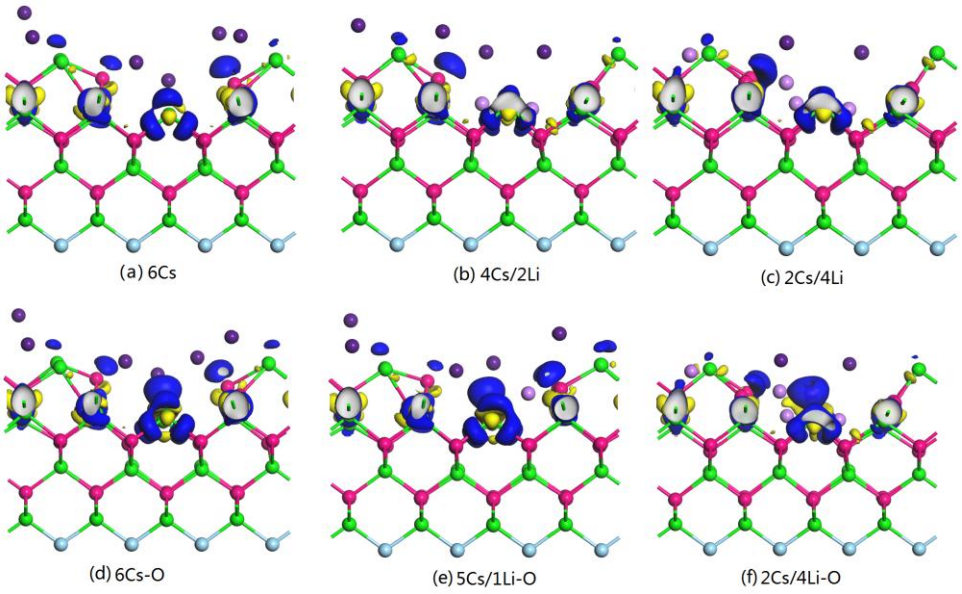

Fig. 2. Electronic density difference of 6Cs, 4Cs2Li, 2Cs4Li, 6Cs-O, 5Cs1Li-O, 2Cs4Li-O models (colour online)

According to Helmholtz equation, surface dipole moment μ can be calculated by $\mu = A\Delta\Phi/12\pi\Theta$ [30], where, A is the area in Å2 per(1×1) surface unit cell, $\Delta\Phi$ is the work function change in eV, Θ is the coverage of adsorbed Cs and Li atoms. The calculated dipole moment μ of different models were shown in table 1. A negative μ showed that the dipole moment directed from substrate layer to adsorbed atoms. The addition of O atom increased the dipole moment, thereby lowering the work function. After the addition of Li atom, the dipole moment first increased and then decreased, and the maximum value will be reached when the ratio of Cs: Li atom is 4:2 and 5:1 respectively in the process of Cs only activation process and Cs/O activation process.

According to the research of Hogan et al [31], the nature of the adsorption-induced dipoles can be analyzed by considering the charge redistribution after adsorption. In this method, the charge variation $\Delta\rho$ (r) of the adsorption model is defined as a function of spatial position:

$$\Delta\rho(\mathbf{r}) = \rho_{ad}(\mathbf{r}) + \rho_{GaAs}(\mathbf{r}) - \rho_{ad/GaAs}(\mathbf{r}) \tag{3}$$

where, ρ_{GaAs} and $\rho_{ad/GaAs}$ are respectively the total electron density (ρ >0) of the relaxed models before and after adsorption, ρ_{ad} is the electron density of the isolated adsorbed unit. In analogy to the concept of center-of-mass, the following quantities are calculated by:

$$\begin{aligned} Q^{+} &= \sum_i \Delta\rho(\mathbf{r}_i) \quad \text{for} \quad \Delta\rho(\mathbf{r}_i) > 0 \\ Q^{-} &= \sum_i \Delta\rho(\mathbf{r}_i) \quad \text{for} \quad \Delta\rho(\mathbf{r}_i) < 0 \end{aligned} \tag{4}$$

$$Q^{\pm} = Q^{+} + Q^{-} \tag{5}$$

$$d_z = \left.\frac{\sum_i \Delta\rho(\mathbf{r}_i) z}{Q^{+}}\right|_{\Delta\rho(\mathbf{r}_i)>0} - \left.\frac{\sum_i \Delta\rho(\mathbf{r}_i) z}{Q^{-}}\right|_{\Delta\rho(\mathbf{r}_i)<0} \tag{6}$$

where, the quantities $Q^{\pm}$ and d_z respectively represent the average dipole charge and the average dipole length normal to the surface, the summations run over a mesh of points $\{\mathbf{r}_i\}$ describing the whole slab supercell, z indicates the coordinate value along z axis (labeled in Fig.1, z=0 is defined at the bottom of the clean surface model). The average dipole moment is calculated as $p_z = \left|Q^{\pm}\right| \times d_z$. The calculated $\left|Q^{\pm}\right|$, d_z and p_z were collected in Table 1. Results showed that the addition of O atom increased the amount of charge transfer, which was because the electronegativity of O, Cs and Li was 3.44, 0.79 and 0.98 respectively, the addition of O element caused Cs and Li to lose electrons further, resulting in the increase of dipole charge. The addition of O atom reduced the length of dipole moment, this was due to the increase in charge transfer caused by O atoms mainly occurred in a small region near O, so the dipole moment decreased.

The length of the dipole moment decreased as the number of Li atoms increased. This occurred because the adsorption position of the Li atoms was closer to the surface, leading to a shorter dipole moment. Upon introducing the Li, the amount of charge transfer initially increased and subsequently decreased. This behavior could be attributed to the fact that when a small number of Li atoms replaced Cs atoms, they adsorbed closer to the surface and were more prone to charge transfer, thereby increasing the charge transfer amount. As the number of Li atoms increased, the charge transfer on the surface gradually saturated. Due to their lower electronegativity and large radius, Cs atoms exhibited a higher propensity for charge transfer compared to Li atoms. Consequently, the amount of charge transfer first increased and then decreased with the addition of Li atoms. The results of p_z calculations indicated that as the number of Li atoms increased, p_z first increased and then decreased, reaching its maximum value in the 4Cs/2Li and 5Cs/1Li-O models. These calculated results were consistent with those obtained from work function calculations.

3.3. Band structure and partial density of states

The band structure of clean, 6Cs, 4Cs/2Li, Cs-O and 5Cs/1Li-O adsorbed surface models were depicted in Fig.3, with lowest work function, 4Cs/2Li and 5Cs/1Li-O were chosen in the analysis of Cs/Li activation and Cs/Li-O activation respectively. Results showed that after Cs activation, the band gap became slightly wider, both CBM and VBM move towards the low energy end, which made the excitation of photoelectrons easier, CBM level were highly localized. The introduction of Li atom reduced the localization of the CBM, CBM and VBM moved to the low energy end, and the band gap was narrowed. Compared with Cs adsorption alone, VBM and CBM moved towards the low energy end, the band gap was narrowed. During Cs-O activation, the introduction of Li atom enhanced the localization of VBM, VBM and CBM moved to the high energy side.

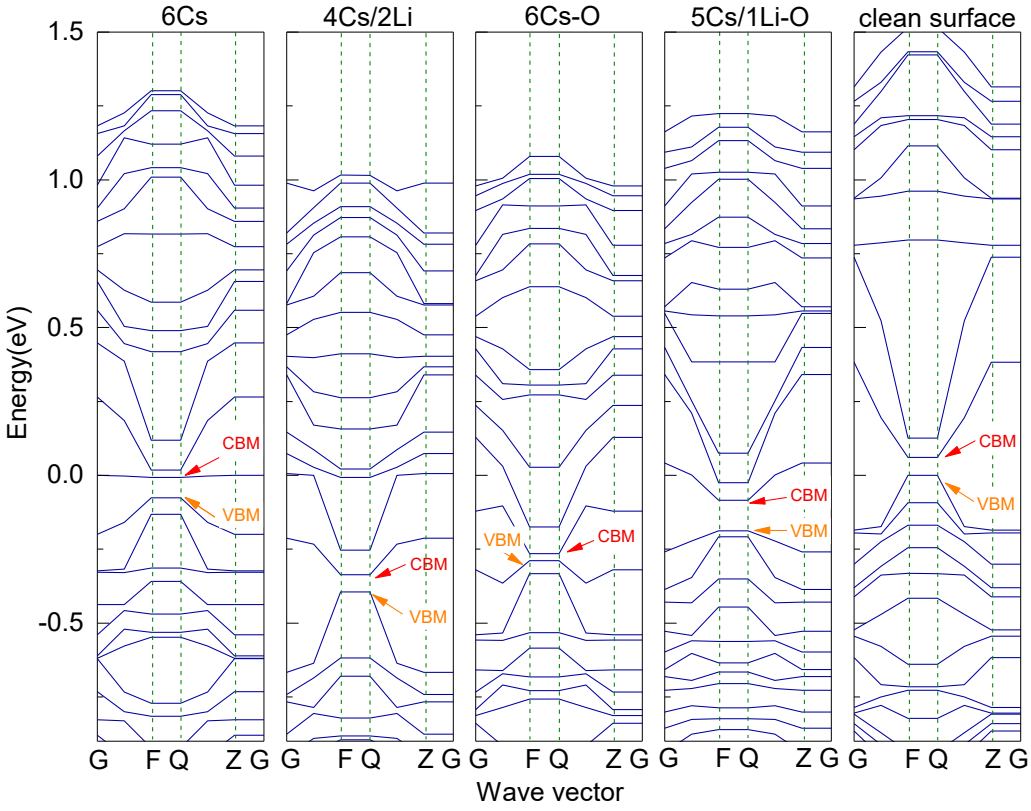

Fig. 3. Band structure of clean, 6Cs, 4Cs/2Li, Cs-O and 5Cs/1Li-O adsorbed surface models (colour online)

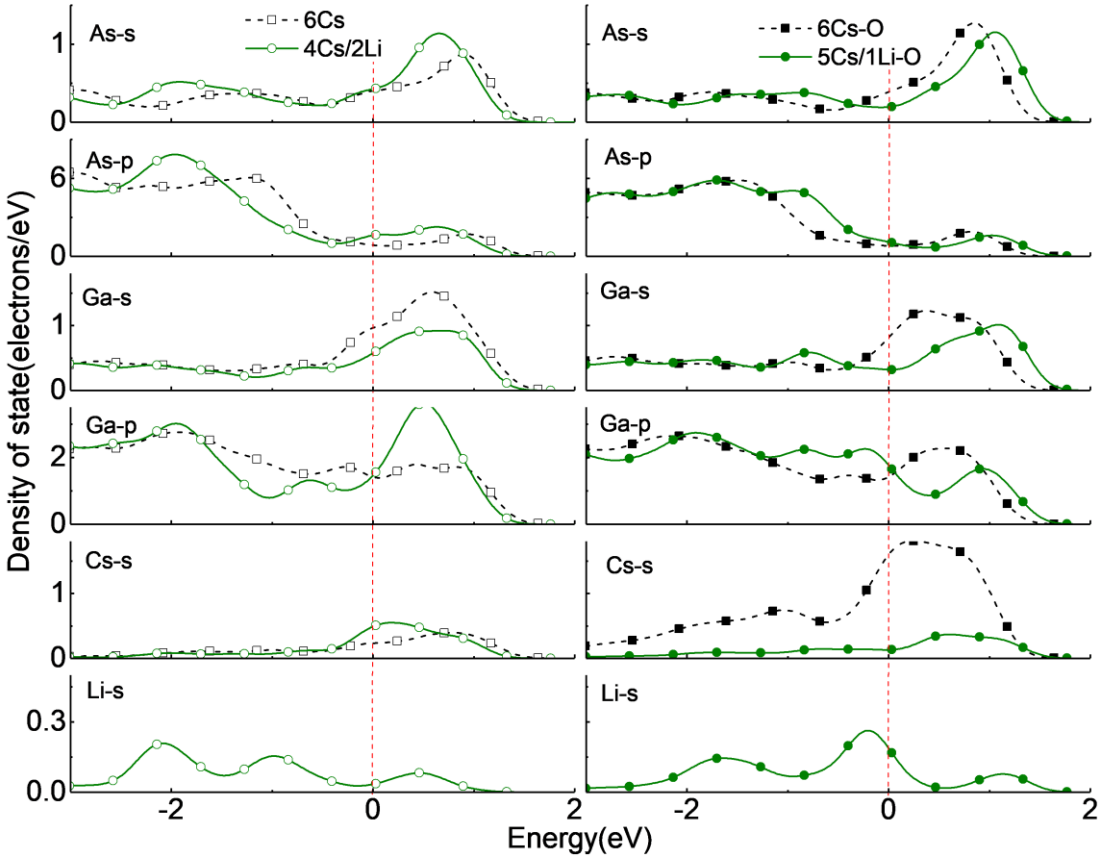

Fig. 4. PDOS of clean, 6Cs, 4Cs/2Li, Cs-O and 5Cs/1Li-O adsorbed surface models (colour online)

In order to investigate the causes of band structure changes, the partial density of state (PDOS) curves was shown in Fig. 4. The left and right panels represented the PDOS curves of the adsorption models without and with O atoms respectively. Similar to the band structure diagram, the configurations of 4Cs/2Li and 5Cs/1Li-O are selected to analyze the O-free and O-contained activation processes. In the clean surface model, the CBM was primarily contributed from As s, Ga s, and Ga p states, while the VBM was mainly contributed by As p states, when Cs atoms were introduced, these electronic states shifted toward the lower energy end, resulting in both the VBM and the CBM moving toward the low-energy region, compared to the Cs only adsorbed model, Li atoms in the Cs/Li model caused the As p state move towards the lower-energy end, the DOS of As p at VBM was increased, causing the movement of VBM towards the lower-energy end, the Ga s state was lowered and moved towards the high-energy side, the DOS of As s state was increased and barely moved, the contribution of Ga p state to VBM was obviously increased.

Compared to the Cs only adsorbed model, the introduction of O atom in 6Cs-O model caused the As s and Ga p state increase obviously and the move towards lower energy side, inducing the downward movement of VBM. As p state was slight decreased and moved towards lower energy side, causing the downwards movement of CBM. The increase in Ga s, As s, Ga p state density at the CBM facilitated photoemission. The introduction of the O atom significantly enhanced the contribution of the Cs s state to both the VBM and CBM. In the process of Cs-O activation, the introduction of Li atoms caused As s, As p, Gas, and Ga p states to shift toward the high-energy end, while both the VBM and CBM moved upward. In the 6Cs-O adsorbed model, upon the introduction of the Li atom, the Cs s state exhibited a significant decrease, which suggested that the incorporation of the Li atom facilitated the transfer of electrons from the Cs s state, the incorporation of the Li element induced shifts in the VBM and CBM, facilitating the transfer of electrons from the Cs s state. This process enhanced the dipole moment and effectively promoted photoemission.

Compared to the clean surface, the electronic changes for each state were presented in Table 2, for Cs, Li and O atoms, the total number of all the state was collected in the table. As can be observed from the table, the Ga s state of each adsorption model decreased, whereas the Ga p, As s, and As p states increased, with the exception of a slight decrease of As s state in the 5Cs/1Li model. Due to the cleavage of chemical bonds on the clean surface, the original sp^3 hybrid orbital exhibited a tendency to transform into an sp^2 hybrid orbital. After activation, the surface typically demonstrated an increase in p state density, a decrease in s state density, and a recovery of the sp^2 hybrid orbital to an sp^3 hybrid orbital.

When Cs atoms were introduced independently, more than half of the electrons from the Cs atoms were transferred to the surface states of Ga p, As s, and As p. This transfer resulted in the formation of a dipole moment, which enhanced the photoemission process. After a small number of Li atoms were introduced, the amount of charge transfer on Cs atoms increased significantly. Despite the fact that Li atoms were less electronegative and had a smaller radius, which was generally unfavorable for charge transfer, they exhibited greater charge transfer compared to Cs atoms in the 6Cs model due to their proximity to the surface. The incorporation of a small number of Li atoms during Cs-O activation could result in O atoms acquiring fewer electrons, thereby enabling a greater transfer of electrons to the surface. When an oxygen atom is incorporated into the 6Cs model, a portion of the electrons from the cesium atoms were transferred to the O atom. This transfer reduced the number of electrons got by the Ga p, As s, and As p states previously. Since both Cs and Li in 5Cs/1Li-O lost a greater number of electrons compared to Cs in 6Cs-O, the charge transfer was more significant.

Table 2. The change of various states of 6Cs, 4Cs/2Li,6Cs-O and 5Cs/1Li-O models

	6Cs	4Cs/2Li	6Cs-O	5Cs/1Li-O
Ga s	-5.91%	-6.09%	-6.8%	-4.87%
Ga p	+5.13%	+5.75%	+5.07%	4.93%
As s	+1.02%	+2.36%	+1.21%	-0.13%
As p	+2.41%	+2.29%	+1.59%	1.79%
Cs s+p	-51.33%	-71.5%	-53.17%	-57.6%
Li s+p	--	-57%	--	-62%
O s+p	--		+26%	+25.25%

** "+" represented a percentage increased and "-" represented a percentage decreased*

3.4. Absorption coefficient and reflectivity

The calculated absorption coefficient and reflectivity curves of clean surface, 6Cs, 4Cs2Li, 6Cs-O and 5Cs1Li-O adsorbed models were depicted in Fig.5. An increase in the absorption coefficient could enhance photoemission efficiency, whereas an increase in reflectivity could hinder photons from penetrating the surface to excite photoelectrons. The clean surface exhibited an absorption peak at 3.98 eV, while the adsorption of Cs, Li, and O introduced a new absorption peak in the range of 5~6 eV. Both Cs only adsorbed and co-adsorption systems (Cs/Li, Cs-O, and Cs/Li-O) enhanced the absorption coefficient, thereby promoting photoemission performance. Notably, the 4Cs2Li model demonstrated the most significant improvement in the absorption coefficient.

Analysis of the reflectance curve showed that, compared to the clean surface, the reflective curve of 6Cs model showed a double peak, and the peak value significantly decreases. At this time, the adding of Li atoms could greatly increase the reflectance, affecting the entry of photons into the body to form photoelectric emission. The reflectivity of the 6Cs-O co-adsorption model was slightly higher than that of the 6Cs model. Introducing a small amount of Li atoms into the Cs-O co-adsorption model would cause the reflectivity peak to shift towards the low-energy end and the peak value to decrease, reducing the reflectivity and facilitating the penetration of photons through the surface and into the body to cause photoelectric emission.

In summary, despite the 4Cs2Li model exhibiting a large absorption coefficient which was conducive to photoemission, it also demonstrated a high reflectivity which would hinder photoemission. The reflectivity of the 5Cs1Li-O and 6Cs-O models was decreased by the introduce of O atom, which facilitated the passage of photons through the surface and is conducive to photoemission, additionally, the increased absorption coefficients of these two models further enhanced their photoemission properties.

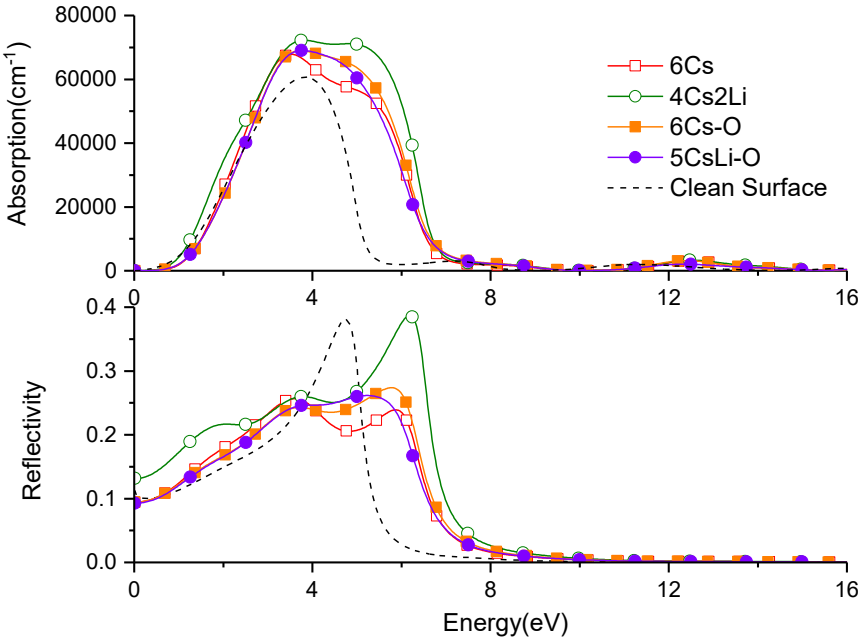

Fig. 5. Absorption coefficient and reflectivity of typical models (colour online)

4. Conclusion

In this work, DFT with plane-wave ultrasoft pseudopotential based on first-principles was used to investigate the Cs/Li-O co-adsorption on the GaAs(001)β2 (2×4) reconstruction surface. Firstly, the structural distortion, stability, and ionicity were analyzed. Subsequently, the photoemission properties were investigated in detail from three perspectives: dipole moment, band structure, and optical properties. Results showed that:

(I)The adsorption of O and Li atoms exacerbated the lattice distortion. The calculation results showed that the photocathode life can be increased by adding O and Li atoms. The ionicity of oxygen-containing model was stronger than that of oxygen-free model.

(II)Work function results showed that during Cs only activation and Cs/O activation, the proper introduction of Li atoms could improve the photoemission, but it should be noted that the introduction of too much Li atoms would reduce of photoemission. The change of work function was mainly caused by the dipole moment formed by the transfer of electrons from Cs and Li atoms to the surface. The adsorption of O and Li atoms enhanced the charge transfer and reduced the distance between positive and negative charge centers. In both the O-containing and O-free models, the dipole moment initially increased and subsequently decreased as the number of Li atoms increased, achieving its maximum value in the 4Cs2Li and 5Cs1Li-O models, respectively.

(III)After activation, the surface typically demonstrated an increase in p state density, a decrease in s state density, and a recovery of the sp^2 hybrid orbital to an sp^3 hybrid orbital. The CBM was primarily contributed from As s, Ga s, and Ga p states, while the VBM was mainly contributed by As p states, the variations in these states leaded to the movement of the VBM and CBM.

(IV)Despite the 4Cs2Li model exhibiting a large absorption coefficient which was conducive to photoemission, it also demonstrated a high reflectivity which would hinder photoemission. The reflectivity of

the 5Cs1Li-O and 6Cs-O models was decreased by the introduce of O atom, which facilitated the passage of photons through the surface and is conducive to photoemission, additionally, the increased absorption coefficients of these two models further enhanced their photoemission properties.

Acknowledgements

Support from Shanxi Provincial Basic Research Program (Exploratory Class) Youth Project (202303021212262), Yuncheng University Doctoral Startup Fund (YQ-2023065).

References

[1] B. Bouabdallah, Y. Bourezig, Y. Brahimi, Journal of Materials Processing Technology **209**(3), 1495 (2019).
[2] S. Karkare, L. Boulet, L. Cultrera, B. Dunham, X. Liu, W. Schaff, I. Bazarov, Physical Review Letters **112**, 097601 (2016).
[3] A. Luque, A. Marti, C. Stanley, Nature Photonics **6**, 146 (2012).
[4] R. M. Balagula, M. Jansson, M. Yukimune, J. E. Stehr, F. Ishikawa, W. M. Chen, I. A. Buyanova, Scientific Reports **10**, 8216 (2020).
[5] S. Manna, H. Huang, S. F. C. D. Silva, C. Schimpf, M. B. Rota, B. Lehner, T. Reindl, A. Rastelli, Applied Surface Science **532**, 147360 (2020).
[6] Y. Zhang, B. Chang, J. Zhao, F. Shi, H. Cheng, Applied Physics Letters **99**, 101104 (2011)
[7] Y. Diao, L. Liu, S. Xia, Applied Nanoscience **10**, 807 (2020).
[8] V. L. Alperovich, A. G. Paulish, H. E. Scheibler, A. S. Terekhov, Applied Physics Letters **66**, 2122 (1995)
[9] D. A. Orlov, C. Krantz, A. Wolf, A. S. Jaroshevich, S. N. Kosolobov, H. E. Scheibler, A. S. Terekhov, Journal of Applied Physics **106**, 054907 (2009).
[10] Z. Xue, Optoelectronic Technology **1**, 23 (1987).
[11] G. A. Mulhollan, J. C. Bierman, Journal of Vacuum Science and Technology A **26**(5), 1195 (2008)
[12] Y. Sun, R. E. Kirby, T. Maruyama, G. A. Mulhollan, J. C. Bierman, P. Pianetta, Applied Physics Letters **95**(17), 174109 (2009).
[13] L. Liu, Y. Diao, S. Xia, F. Lu, J. Tian, Applied Surface Science **478**, 393 (2019).
[14] M. He, Y. Zhu, S. Zheng, S. Xing, S. Liu, B. Song, J. Optoelectron. Adv. M. **26**(1-2) 42 (2024).
[15] S. Ding, H. Zhang, W. Liu, D. Sun, Q. Zhang, Journal of Material Science: Materials in Electronics **29**, 11878 (2018).
[16] J. Perdew, K. Burke, M. Ernzerhof, Physical Review Letters **77**, 3865 (1996)
[17] A. Bouhemadou, K. Haddadi, S. Bin-Omran, R. Khenata, Y. Al-Douri, S. Maabed, Materials Science in Semiconductor Processing **40**, 64 (2015).
[18] X. Yu, Z. Jin, G. Shao, Journal of Material Science: Materials in Electronics **33**, 2335 (2022).
[19] G. Kresse, J. Hafner, Physical Review B **47**, 558 (1993).
[20] B. Sieber, J. L. Farvacque, J. Wang, J. W. Steeds, Materials Science and Engineering B **20**, 29 (1993).
[21] W. Wang, G. Lee, M. Huang, R. M. Wallace, K. Cho, Journal of Applied Physics **107**, 103720 (2010).
[22] S. Krukowski, P. Kempisty, P. Strak, Journal of Applied Physics **105**, 113701 (2009).
[23] M. G. Brik, C. G. Ma, V. Krasnenko, Surface Science **608**, 146 (2013).
[24] J. Zou, B. Chang, Z. Yang, Y. Zhang, J. Qiao, Journal of Applied Physics **105**, 013714 (2009).
[25] F. Machuca, Y. Sun, Z. Liu, Journal of Vacuum Science and Technology B **18**, 3042 (2000).
[26] J. R. Kitchin, Physical Review B **79**, 205412 (2009).
[27] L. Schimka, L. Harl, A. Stroppa, A. Grüneis, M. Marsman, F. Mittendorfer, G. Kresse, Nature Materials **9**, 741 (2010).
[28] P. Mori-Sánchez, A. M. Pendás, V. Luaña, Journal of Americal Chemical Society **124**(49), 14721 (2002).
[29] A. L. Rosa, J. Neugebauer, Physical Review B **73**, 205346 (2006).
[30] W. X. Li, C. Stampfl, M. Scheffler, Physical Review B **65**, 075407 (2002).
[31] C. Hogan, D. Paget, Y. Garreau, M. Sauvage, G. Onida, L. Reining, P. Chiaradia, V. Corradini, Physical Review B **68**, 205313 (2003).

*Corresponding author: 624554818@qq.com